

# **$Z$ -dependent Barriers in Multifragmentation from Poissonian Reducibility and Thermal Scaling**

L. Beaulieu, L. Phair, L.G. Moretto and G.J. Wozniak

*Nuclear Science Division, Lawrence Berkeley National Laboratory, Berkeley, California 94720*

(May 16, 2018)

## **Abstract**

We explore the natural limit of binomial reducibility in nuclear multifragmentation by constructing excitation functions for intermediate mass fragments (IMF) of a given element  $Z$ . The resulting multiplicity distributions for each window of transverse energy are Poissonian. Thermal scaling is observed in the linear Arrhenius plots made from the average multiplicity of each element. “Emission barriers” are extracted from the slopes of the Arrhenius plots and their possible origin is discussed.

arXiv:nucl-ex/9805002v1 13 May 1998

Emission of multiple intermediate mass fragments (IMF),  $3 \leq Z \leq 20$ , is an important decay mode in heavy-ion collisions between 20A and 100A MeV [1,2]. Despite extensive studies, the nature of the fragmentation process, whether statistical or dynamical, remains an open problem. An historic overview of low energy reactions shows that the emission probabilities and excitation functions are by far the best observables in distinguishing between statistical processes (dominated by phase space, as in the case of light particle evaporation and fission), and prompt, dynamical processes (like direct reactions) [3]. Indeed, several aspects of nuclear multifragmentation may be understood in terms of *nearly independent* fragment emission from multifragmenting sources with *thermal-like* probabilities [4–9].

It was found [4–6] that the experimental  $Z$  integrated fragment multiplicity distributions  $P_n^m$  are binomially distributed in each transverse energy ( $E_t$ ) window, where  $n$  is the number of emitted fragments and  $m$  is the number of throws. The transverse energy  $E_t$  is calculated from the kinetic energies  $E_i$  of all the charged particles in an event and their polar angles  $\theta_i$ , as  $E_t = \sum_i E_i \sin^2 \theta_i$ . The extracted one-fragment emission probabilities  $p$  give linear Arrhenius plots (i.e. excitation functions) when  $\log 1/p$  is plotted vs  $1/\sqrt{E_t}$ . If the excitation energy  $E^*$  is proportional to  $E_t$  and consequently, the temperature  $T$  to  $\sqrt{E_t}$ , these linear Arrhenius plots suggest that  $p$  has the Boltzmann form  $p \propto \exp(-B/T)$  [4–6].

Similarly, the charge distributions for each fragment multiplicity  $n$  are observed to be reducible to a single charge distribution and to be thermally scalable [7,8]. Also, the experimental particle-particle angular correlation is reducible to the individual fragment statistical angular distributions and thermally scalable [9].

The appeal of this comprehensive picture is marred by a number of open problems. One problem, which will be dealt with here, is that the binomial decomposition has been performed on the  $Z$ -integrated fragment multiplicities, typically associated with  $3 \leq Z \leq 20$ . Thus, the Arrhenius plot generated with the resulting one fragment probability  $p$  is an average over a range of  $Z$  values. Fortunately, it has been shown that the Arrhenius plots should survive such a  $Z$  averaging, and yield an effective “barrier” (slope) dominated by the lowest  $Z$  value [4–6]. However, this procedure clearly implies a substantial loss of

information, and renders the binomial parameters  $p$  and  $m$  difficult to interpret.

In light of the above considerations, an analysis of the multiplicities for each fragment  $Z$  value may solve many of these difficulties. Furthermore, it has been pointed out that a binomial distribution could be distorted by the averaging associated with the transformation  $E^* \rightarrow E_t$  leading to possibly incorrect values of  $m$  and  $p$  [10]. However, it has been shown that, while  $p$  and  $m$  separately can conceivably be distorted by the transformation, the average multiplicity  $\langle n \rangle = mp$  is far more resistant to the averaging process [10,11]. It would be useful if a way could be found of avoiding the individual extraction of  $p$  and  $m$  while retaining the possibility of constructing an Arrhenius plot.

In this letter, we analyze the experimental fragment multiplicity distributions for each individual fragment  $Z$  value. We show that they are Poissonian. The associated mean multiplicities for *each*  $Z$  give linear Arrhenius plots from which the corresponding  $Z$  dependent barriers can be extracted. The physical dependence of these barriers on  $Z$  may shed light on the fundamental physics associated with multifragmentation, as fission barriers have done for the fission process.

The effect of restricting the fragment definition to a single  $Z$  value is rather dramatic. In Fig. 1, ratios of the variance to the mean as a function of  $E_t$  are given for a number of  $Z$  values, and for the case  $Z \geq 3$  [6]. For individual  $Z$  values the ratios are very close to one, while for the  $Z$  integrated case there is a sagging at large  $E_t$ . The explanation for these features can be found by recalling that for a binomial distribution

$$\langle n \rangle = mp; \quad \sigma^2 = mp(1 - p); \quad \frac{\sigma^2}{\langle n \rangle} = 1 - p. \quad (1)$$

For  $p \rightarrow 0$ , the ratio  $\sigma^2 / \langle n \rangle \rightarrow 1$ . This is the Poisson limit. When extensive summation over  $Z$  is carried out, the elementary probability  $p$  increases sufficiently at the highest values of  $E_t$  so that the Poisson distribution is replaced by the more general binomial distribution. On the other hand, the restriction to any given  $Z$  value decreases the elementary probability  $p$  so dramatically that the above ratio effectively remains unity at all values of  $E_t$  and the distributions become Poissonian:

$$P_n(Z) = \frac{\langle n \rangle^n e^{-\langle n \rangle}}{n!}, \quad (2)$$

where  $\langle n \rangle$  is  $\langle n \rangle (E_t)$ . We show the quality of the Poisson fits to the multiplicity distribution in Fig. 2. These Poisson fits are excellent for all  $Z$  values starting from  $Z=3$  up to  $Z=14$  over the entire range of  $E_t$  and for all the reactions which we have studied. Thus we conclude that reducibility (we should call it now Poissonian reducibility) is verified at the level of individual  $Z$  values for many different systems. Incidentally, for the Xe induced reactions, there is an excellent overlap of the data sets for different targets as a function of  $E_t$ . They all follow the Poisson fit to the Au target data. The probabilities  $P_n$  and the range of  $E_t$  increase with the increasing target mass from V to Au, as they must if  $E_t$  is a reasonable measure of the dissipated energy.

The experimental observation of Poissonian reducibility directly implies that IMF production is dominated by a stochastic process. Of course stochasticity falls directly in the realm of statistical decay, either sequential or simultaneous (see section 5.5 of ref. [6] or ref. [12]). It is less clear how it would fare within the framework of a dynamical model.

In order to verify thermal scaling i.e. if the emission probabilities are thermal, we generate Arrhenius plots by plotting  $\log \langle n \rangle$  vs  $1/\sqrt{E_t}$ . Here, as in previous works, we assume that  $E_t \propto E^*$  and that  $E^* \propto T^2$ , according to the simplest strongly degenerate Fermi gas dependence at constant volume. We are of course aware that high excitation energies and/or lower densities can lead to deviations, which may well be looked for in the future. We expect  $\langle n \rangle$ , like  $p$ , to be of the form  $\langle n \rangle = F(T, \dots)e^{-B/T}$ , where the specific form of the pre-exponential factor depends ultimately on whether a reaction theory or a chemical equilibrium description will prevail. We use the Arrhenius plot in the traditional spirit of evidentiating the leading  $T$  dependence contained in the exponential. The top four panels of Fig. 3 gives a family of these plots for four different reactions. Each family contains  $Z$  values extending from  $Z=3$  to  $Z=14$ . The observed Arrhenius plots are strikingly linear, and their slopes increase smoothly with increasing  $Z$  value. One slight exception is the large  $Z$  ( $\geq 10$ ) data for Xe+Cu. At high  $E_t$ , the data deviates from the linear dependence observed elsewhere.

For this smaller system, it is conceivable that charge conservation constraints lead to this behaviour. The overall linear trend demonstrates that thermal scaling is also present when individual fragments of a specific  $Z$  are considered. Even apart from the linearity of the Arrhenius plots, important information is already contained in the range covered by the yield of individual fragments over the range of  $E_t$  shown in Fig. 3. For processes not dominated by phase space (e.g. low energy direct reactions), one expects the excitation function to depend weakly upon excitation energy. Typically the cross sections vary by factors of a few. In the present data, the mean multiplicity  $\langle n \rangle$  varies with  $E_t$  by one to two orders of magnitudes. This is a strong evidence for the involvement of the internal degrees of freedom typical of high barrier statistical decays.

The advantage of considering individual  $Z$  selected fragments is readily apparent. For any given reaction, both Poissonian reducibility and thermal scaling are verifiable not just once, as in the binomial analysis, but for as many atomic numbers as are experimentally accessible. Take for example the Ar+Au reaction ( $E/A=110\text{MeV}$ ) shown in the top right panel of Fig. 3. For this specific reaction, we can verify both reducibility and thermal scaling for 12 individual atomic numbers. Since there are 29  $E_t$  bins, Poissonian reducibility is tested 29 times for each  $Z$  value, i.e.,  $12 \times 29 = 348$  times for this reaction alone. Including all the cases shown in Fig. 3, we have tested Poissonian reducibility 936 times. This is an extraordinary level of verification of the empirical reducibility and thermal scaling with the variable  $E_t$ .

Two added bonuses arise from this procedure.

1) The criticism has been raised that the linearity of the Arrhenius plots arises from an autocorrelation, since the complex fragments also contribute to  $E_t$  [13]. In the present analysis this criticism can be dismissed, since each individual  $Z$  contributes a vanishingly small amount to  $E_t$  ( $\leq 5\%$ ), even in the region of maximum yields. Still, to be sure that there is no autocorrelation in Fig. 3, we have repeated the analysis, for Xe+Au at 50A MeV, by: i) removing from  $E_t$  the contribution of the individual  $Z$  ( $E_t^Z$ ) that we have selected (Fig. 3, bottom left panel); ii) by using only the  $E_t$  of the light charge particles,  $E_t^{LCP}$

(Fig. 3, bottom right panel) . In both cases, the Arrhenius plots remain linear over almost the entire range of  $E_t$  and cover 1 to 2 orders of magnitude. Quantitatively, the rate of change of the slopes with  $Z$  remains the same regardless of the definition of  $E_t$ , as shown in the top panel of Fig. 4. This behaviour is expected if the slopes are related to some physical barriers.

In our attempt to avoid autocorrelation by excluding from  $E_t$  all IMFs ( $E_t^{LCP}$ ) or the  $Z$  value under investigation ( $E_t^Z$ ), we have introduced another kind of distortion. Excluding from  $E_t$  all fragments of charge  $Z$  to produce  $E_t^Z$  necessarily requires that for those events where  $E_t^Z \approx E_t$ , the yield  $n_Z \rightarrow 0$ . This produces the visible turnover of the Arrhenius plots in the bottom panels of Fig. 3 (the same argument also applies to  $E_t^{LCP}$ ). It has been verified experimentally that the maximum values of the new  $E_t$  scale do indeed correspond to events in which the contribution from a given  $Z$  (or all IMFs) is absent.

2) The extracted elementary probability is now  $\langle n \rangle = \langle mp \rangle$  which, contrary to  $p$  and  $m$ , is very resilient to any averaging associated with the transformation from  $E^*$  to  $E_t$  [10,11].

It may be worth reminding the reader that this procedure does not contradict binomial reducibility. To the contrary, it represents its natural limit for small values of  $p$ , and it expands its applicability by considering each  $Z$  value individually. In going from binomial to Poissonian distributions, the price one pays is the loss of the parameter  $m$ . While in many ways this is a convenient result, it actually implies a loss of scale. In the time sequential interpretation of multifragmentation [6] this implies a loss of information about the time window during which multifragmentation occurs in units of the natural channel period, or the unit time to which the elementary probability is referred. In the spacial interpretation, one loses information about the total mass of the source [6].

Poissonian reducibility and thermal scaling do not contradict recent observations regarding the role of reaction dynamics in the *formation* of the hot primary sources [14–19]. In particular, the experimental scaling is not affected by the presence of multiple sources [6] and the analysis presented here is a powerful test to establish the degree of thermalization in the late stage of the reaction. Kinematic variables seem to retain spatial-temporal in-

formation about the reaction dynamics [15–20] while the associated emission probabilities seem to demonstrate, as verified nearly a 1000 times in the present work, the role of phase space in describing the decay of the sources.

Returning to the Arrhenius plots for individual atomic numbers, it is straightforward to obtain the values of the slopes from Fig. 3 as a function of  $Z$ . The interpretation of these slopes as “emission barriers” is very tempting. If we had the correct excitation energy, rather than  $E_t$ , we could obtain the actual barriers as a function of  $Z$ . Unfortunately we are limited to our running variable  $E_t$ , and to the assumption of its proportionality to  $E^*$ . However, the many linear Arrhenius plots shown here cannot be easily explained without invoking this proportionality. Therefore, with the necessary caution, we explore the possible meaning of these “barriers”. A plot of these barriers as a function of  $Z$  is potentially rich in information. The extracted barriers are shown in Fig. 4 (bottom panel). The barriers appear to increase linearly with  $Z$  at low  $Z$  values and tend to sag below linearity at higher ones.

One could wonder about the role of surface energy on the origin of these barriers. Fragments might be thought as forming by coalescence into a relatively cold and dense nuclear drop out of a hot diluted source. The appearance of a substantial surface energy for the fragment would suggest barriers proportional to  $Z^{2/3}$  ( $A^{2/3}$ ). If this were true, then one would expect the barrier for each  $Z$  to be nearly independent of the system studied. Unfortunately, since the relation between  $E_t$  and excitation energy is unknown, the absolute values of our barriers are also unknown. By normalizing all systems at  $Z=6$  and using the Xe+Au at  $E/A=50$  MeV as the reference, one observes barriers that are indeed fairly independent of the system (Fig. 4, bottom panel). Another possibility is to compare the dependence of the barriers on  $Z$  to that of the conditional barriers measured at low energy [21] (black dots). Their similarity with the multifragmentation barriers is dramatically illustrated. While the Coulomb-like  $Z$  dependence of these barriers is suggestive, we should remark that these are emission barriers rather than Coulomb barriers. Thus the dominance of the Coulomb term is by no means obvious.

In conclusion, Poissonian reducibility and thermal scaling of individual fragments of a given  $Z$  have been observed experimentally for several different systems at bombarding energies ranging from 50 to 110 MeV/nucleon. The high level of verification strongly supports the stochastic/statistical nature of fragment production and provides a clear signal for source(s) thermalization in the late stage of the reaction. Slope parameters were extracted from the Arrhenius plots. The interpretation of these slopes as emission barriers, originating either from Coulomb or surface terms, or both, still needs to be explored. If the physical significance of these  $Z$  dependent “barriers” must remain lamentably open, there is at least the distinct possibility that important physical information is contained therein. Data with isotopically resolved light charged particles and IMFs are needed to further investigate these phenomena.

#### Acknowledgements

This work was supported by the Director, Office of Energy Research, Office of High Energy and Nuclear Physics, Nuclear Physics Division of the US Department of Energy, under contract DE-AC03-76SF00098. One of us (L.B) acknowledge a fellowship from the National Sciences and Engineering Research Council (NSERC), Canada.



## REFERENCES

- [1] B. Borderie, Ann, de Phys. **17**, 349 (1992).
- [2] L.G. Moretto and G.J. Wozniak, Ann. Rev. Nucl. Part. Sci. **43**, 379 (1993).
- [3] L.G. Moretto, Phys. Rev. **179**, 1176 (1969).
- [4] L.G. Moretto *et al.*, Phys. Rev. Lett. **74**, 1530 (1995).
- [5] K. Tso et al., Phys. Lett. B **361**, 25 (1995).
- [6] L.G. Moretto, *et al.*, Phys. Rep. **287**, 249 (1997).
- [7] L. Phair et al., Phys. Rev. Lett. **75**, 213 (1995).
- [8] L.G. Moretto et al., Phys. Rev. Lett. **76**, 372 (1996).
- [9] L. Phair *et al.*, Phys. Rev. Lett **77**, 822 (1996).
- [10] J. Toke *et al.*, Phys. Rev. C **56**, R1683 (1997).
- [11] L. Phair *et al.*, to be published.
- [12] A.S. Botvina and D.H.E. Gross, Phys. Lett. B344, 6 (1995)
- [13] M.B. Tsang *et al.*, Phys. Rev. Lett. **80**, 1178 (1998)
- [14] C.P. Montoya *et al.*, Phys. Rev. Lett **73**, 3070 (1994).
- [15] J. Lukasik *et al.*, Phys. Rev. C **55**, 1906 (1997).
- [16] Y. Larochelle *et al.*, Phys. Rev. C **55**, 1869 (1997).
- [17] J. Toke *et al.*, Phys. Rev. Lett. **75**, 2920 (1995).
- [18] J.F. Lecolley *et al.*, Phys. Lett. B **354**, 202 (1995).
- [19] J.F. Dempsey *et al.*, Phys. Rev. C **54**, 1710 (1996).
- [20] D.R. Bowman *et al.*, Phys. Rev. Lett **70**, 3534 (1993).

[21] K.X. Jing *et al.*, LBNL-40779, submitted to Phys. Rev. C.

## FIGURES

FIG. 1. The ratio of the variance to the mean number of Li, C, O and Ne fragments (solid and open symbols) emitted from the reaction  $^{36}\text{Ar}+^{197}\text{Au}$  at  $E/A=110$  MeV. The star symbols show the same ratio for all IMFs ( $3 \leq Z \leq 20$ ).

FIG. 2. The excitation functions  $P_n$  for carbon (left column) and neon emission (right column) from the reactions  $^{36}\text{Ar}+^{197}\text{Au}$  at  $E/A=110$  MeV (top panels) and  $^{129}\text{Xe}+^{51}\text{V}, ^{\text{nat}}\text{Cu}, ^{89}\text{Y}, ^{197}\text{Au}$  (bottom panels). The lines are Poisson fits to the gold target data.

FIG. 3. Middle and upper panels: The average yield per event of different elements (symbols) as a function of  $1/\sqrt{E_t}$ . Bottom panels: The Xe+Au data at 50A MeV are replotted using the transverse energy of all charged particles excluding the  $Z$  that we have selected,  $E_t^Z$  (left), and (right) that only of the light charged particles,  $E_t^{LCP}$ . The lines are fits to the data using a Boltzmann form for  $\langle n_Z \rangle$ .

FIG. 4. Top panel: Slopes of the Arrhenius plots, normalized to  $Z = 6$ , for Xe+Au at 50A MeV as a function of  $Z$  using the indicated definitions of  $E_t$ . Bottom panel: The  $Z$  dependent “barriers” (the slopes of the Arrhenius plots in Fig. 3). The “barriers” have been scaled relative to  $Z = 6$  of the Xe+Au data. Black dots are low energy conditional barriers from ref. [21] normalized to  $Z = 6$  of Xe+Au.

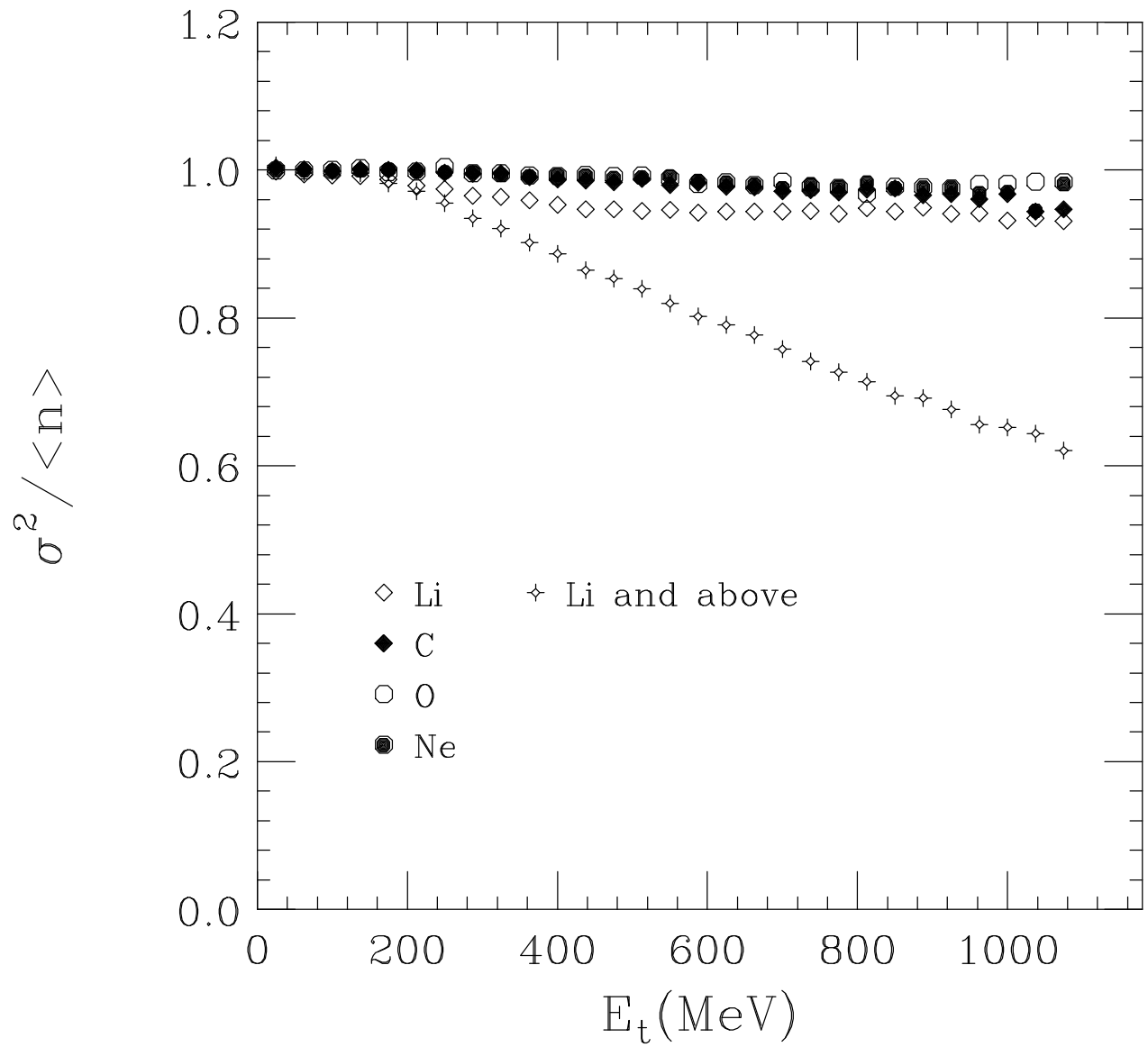


FIG. 1. L. Beaulieu *et al.*

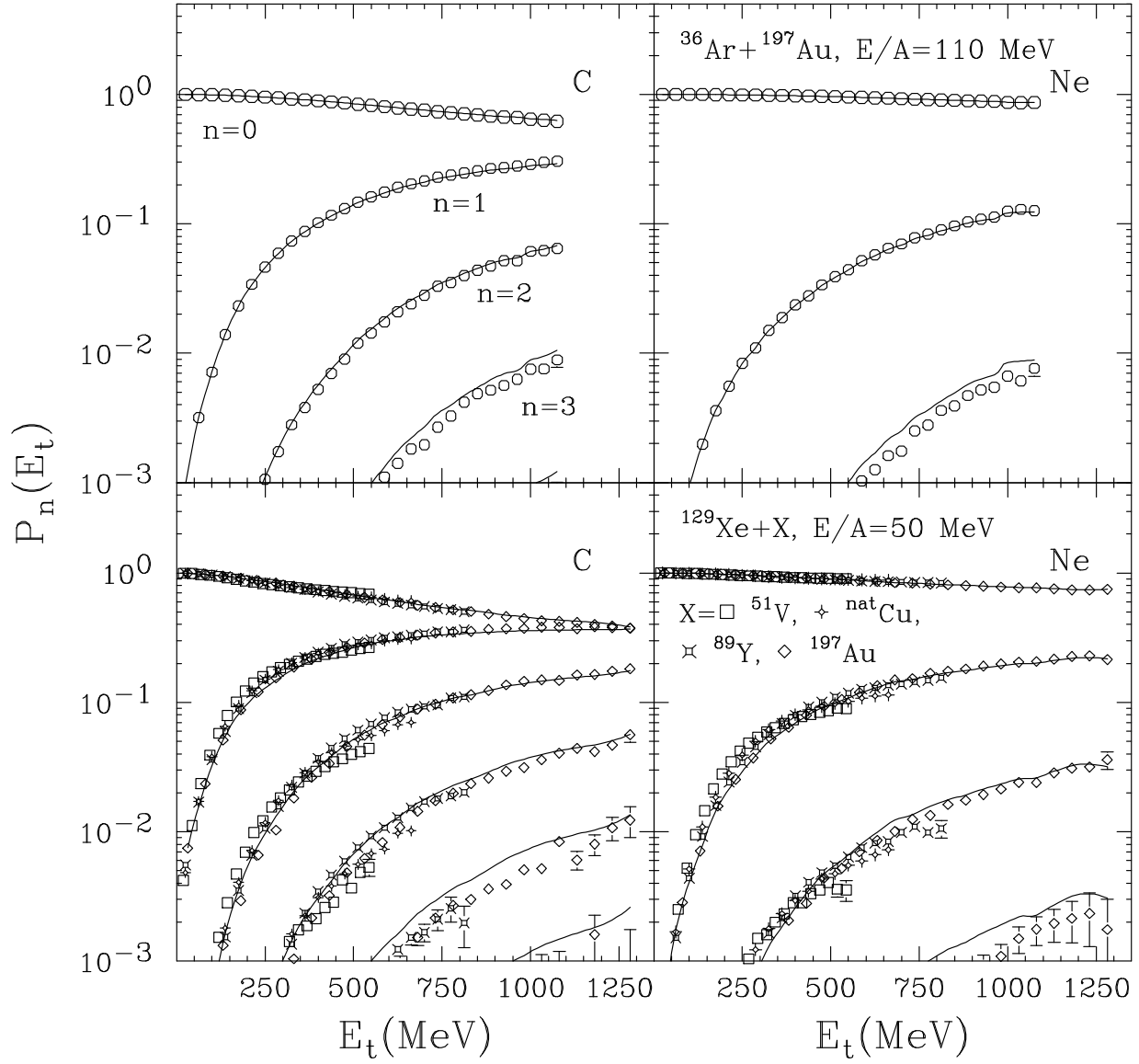


FIG. 2. L. Beaulieu *et al.*

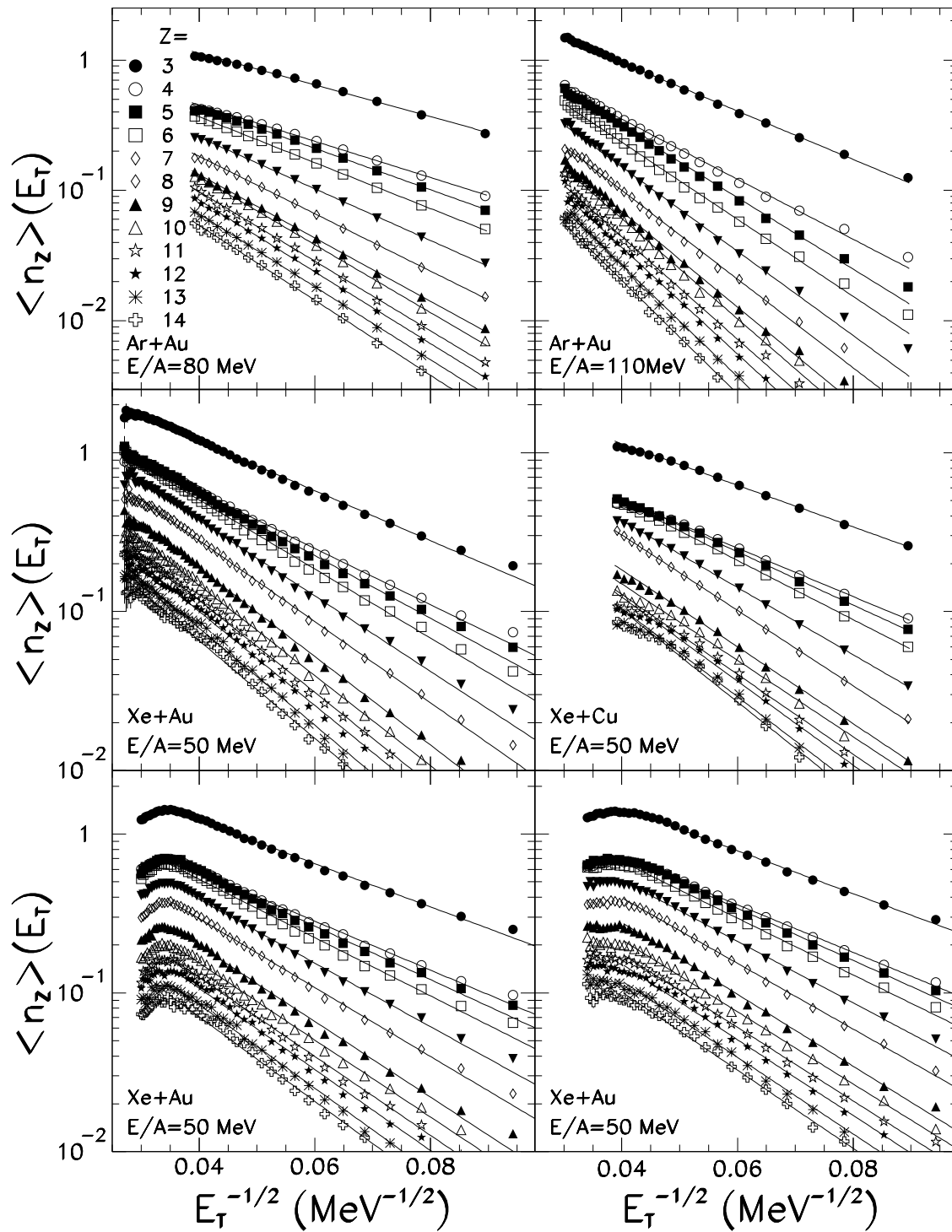


FIG. 3. L. Beaulieu *et al.*

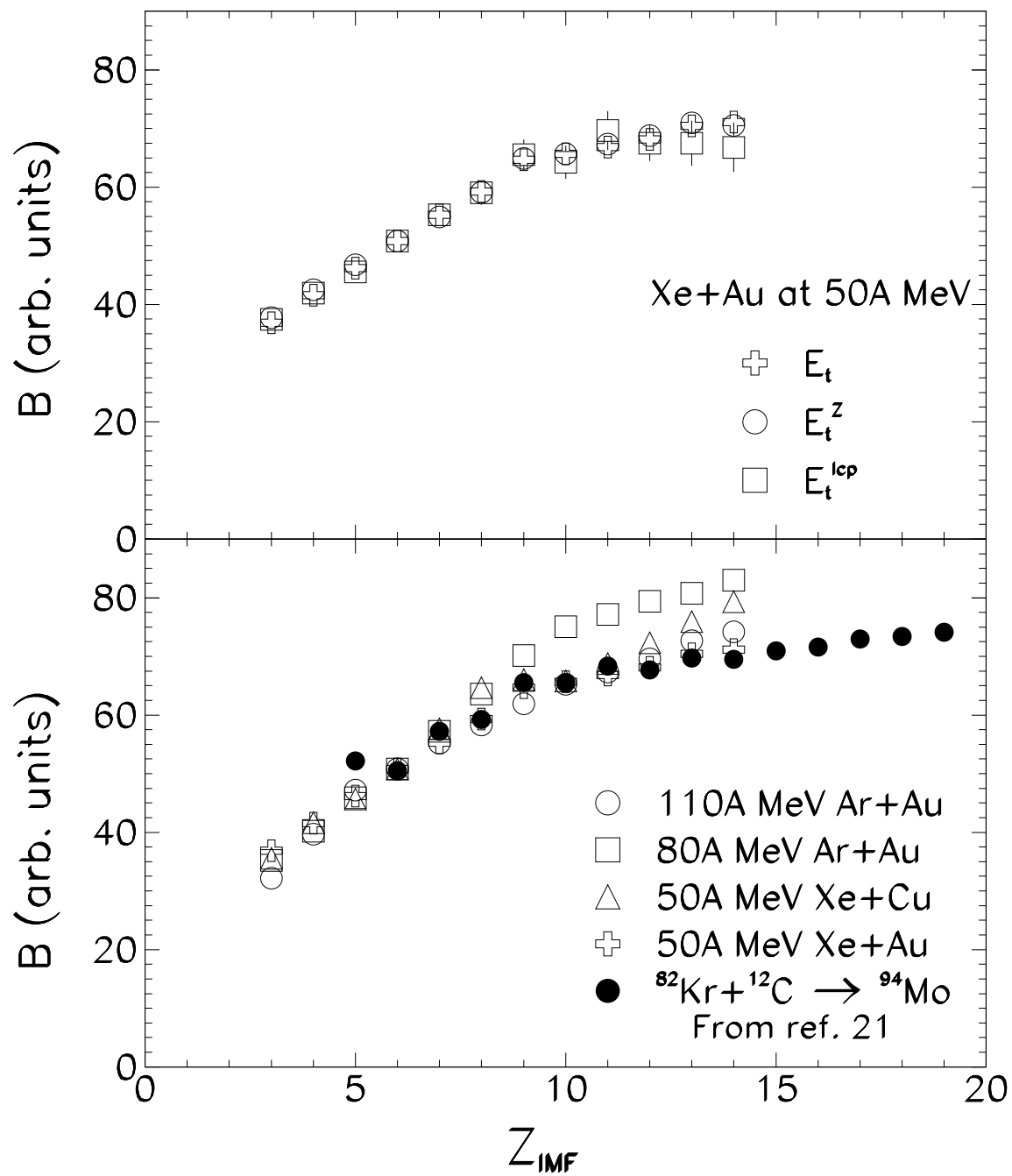


FIG. 4. L. Beaulieu *et al.*